Published OnlineFirst November 30, 2012; DOI: 10.1158/0008-5472.CAN-12-1492

DKK2 Mediates Osteolysis, Invasiveness, and Metastatic Spread in Ewing Sarcoma

Kristina Hauer[1], Julia Calzada-Wack[4], Katja Steiger[4], Thomas G.P. Grunewald[1], Daniel Baumhoer[5], Stephanie Plehm[1], Thorsten Buch[2], Olivia Prazeres da Costa[2], Irene Esposito[3,4], Stefan Burdach[1], and Günther H.S. Richter[1]

Abstract

Ewing sarcoma, an osteolytic malignancy that mainly affects children and young adults, is characterized by early metastasis to lung and bone. In this study, we identified the pro-metastatic gene *DKK2* as a highly overexpressed gene in Ewing sarcoma compared with corresponding normal tissues. Using RNA interference, we showed that DKK2 was critical for malignant cell outgrowth *in vitro* and in an orthotopic xenograft mouse model *in vivo*. Analysis of invasion potential in both settings revealed a strong correlation of DKK2 expression to Ewing sarcoma invasiveness that may be mediated by the DKK effector matrix metalloproteinase 1 (MMP1). Furthermore, gene expression analyses established the ability of DKK2 to differentially regulate genes such as *CXCR4*, *PTHrP*, *RUNX2*, and *TGFβ1* that are associated with homing, invasion, and growth of cancer cells in bone tissue as well as genes important for osteolysis, including *HIF1α*, *JAG1*, *IL6*, and *VEGF*. DKK2 promoted bone infiltration and osteolysis *in vivo* and further analyses defined DKK2 as a key factor in osteotropic malignancy. Interestingly, in Ewing sarcoma cells, DKK2 suppression simultaneously increased the potential for neuronal differentiation while decreasing chondrogenic and osteogenic differentiation. Our results provide strong evidence that DKK2 is a key player in Ewing sarcoma invasion and osteolysis and also in the differential phenotype of Ewing sarcoma cells. *Cancer Res; 73(2); 967–77. ©2012 AACR.*

Introduction

Ewing sarcomas are undifferentiated bone or soft tissue tumors of enigmatic histogenesis mostly occurring in children and adolescents. Genetically, Ewing sarcoma are defined by EWS/ETS translocations (1, 2). These highly malignant tumors frequently arise in bones possibly descending from a mesenchymal stem cell in transition from an undifferentiated state to a more differentiated phenotype of the endothelial, neuroectodermal or, as hypothesized here, of the chondro-osseous lineage (2–4).

Although prognosis of patients with localized disease has markedly improved in past decades, metastatic disease—present in about 25% of patients with Ewing sarcoma at diagnosis—is usually associated with fatal outcome (5, 6). Especially the development of metastases in bones is a catastrophic event in the clinical course of patients with Ewing sarcoma (5, 7). Hence, there is an urgent need to understand the fundamental molecular mechanisms of Ewing sarcoma differentiation, invasion, and osteolytic tumor growth to possibly identify novel therapeutic strategies to prevent metastasis.

Previously, we described an Ewing sarcoma–specific expression signature comprising 37 genes that are highly upregulated or specifically expressed in Ewing sarcoma (8). One of them is dickkopf 2 (Dickkopf, Xenopus, Homolog 2) a member of the dickkopf family. Recently, DKK2 was reported as a key player in stem cell signaling networks due to its function as a Notch signaling target (9). However, its precise cellular function remains elusive. For instance, secreted DKK2 can function as either a Wnt agonist or an antagonist, depending on the cellular context and the expressed amount of its binding partner low-density lipoprotein receptor–related protein 6 (LRP6) and its cofactor Kremen 2 (10–13). In the context of the Wnt/β-catenin pathway, DKK2 may promote osteoclastogenesis by enhancing the expression of osteoclast differentiation factors, thus leading to tumor-associated osteolysis (14, 15). Furthermore, Li and colleagues showed that DKK2

Authors' Affiliations: [1]Children's Cancer Research Center and Department of Pediatrics, Roman Herzog Comprehensive Cancer Research Center and Klinikum rechts der Isar, [2]Institute for Medical Microbiology, Immunology and Hygiene, [3]Institute of Pathology, Technische Universität München, Munich; [4]Institute of Pathology, Helmholtz Center Munich – German Research Center for Environmental Health, Neuherberg, Germany; and [5]Bone Tumor Reference Center at the Institute of Pathology, University Hospital Basel, Basel, Switzerland

Note: Supplementary data for this article are available at Cancer Research Online (http://cancerres.aacrjournals.org/).

This work contains part of the doctoral thesis of K. Hauer.

S. Burdach and G.H.S. Richter share senior authorship.

Corresponding Author: Günther H.S. Richter, Children's Cancer Research Center and Department of Pediatrics, Roman Herzog Comprehensive Cancer Research Center and Klinikum rechts der Isar, Technische Universität München, 81664 Munich, Germany. Phone: 49-89-3068-3235, Fax: 49-89-3068-3791; E-mail: somagene@lrz.tum.de; and guenther.richter@lrz.tum.de

doi: 10.1158/0008-5472.CAN-12-1492

Published OnlineFirst November 30, 2012; DOI: 10.1158/0008-5472.CAN-12-1492

has a role in terminal osteoblast differentiation into mineralized matrices through both canonical Wnt antagonism–dependent and -independent mechanisms (16). On the basis of these observations, we hypothesized that DKK2 is involved in Ewing sarcoma invasion, osteolysis, and chondrogenic/osteogenic differentiation potential.

In the present study, we analyzed the putative oncogenic function of DKK2 in Ewing sarcoma *in vitro* and *in vivo*. We show that DKK2 increases Ewing sarcoma proliferation, anchorage-independent colony formation, osteolysis, and invasiveness, the latter being likely mediated by MMP1. In addition, we show that DKK2 expression prevents neuronal but in parallel enhances chondrogenic and osteogenic differentiation capacity of Ewing sarcoma. Furthermore, DKK2 regulates the expression of different genes important for homing, invasion into bone and osteolysis, suggesting that DKK2 overexpression is a critical factor in Ewing sarcoma malignancy, in particular bone metastasis.

Materials and Methods

Cell lines

Ewing sarcoma lines (MHH-ES1, RD-ES, SK-ES1, SK-N-MC, and TC-71) and neuroblastoma lines (CHP126, MHH-NB11, SHSY5Y, and SIMA) were obtained from the German Collection of Microorganisms and Cell Cultures (DSMZ). Ewing sarcoma line VH64 was kindly provided by Marc Hotfilder (Münster University, Münster, Germany); osteosarcoma cell lines (HOS, HOS-58, MG-63, MNNG, SaOS, SJSA01, U2OS, and ZK-58) by Jan Smida and Michaela Nathrath, Institute of Pathology and Radiation Biology (Neuherberg, Germany). A673 was purchased from ATCC (LGC Standards). SB-KMS-KS1 cells and SB-KMS-MJ1 are Ewing sarcoma cell lines that were established in our laboratory (17, 18). Retrovirus packaging cell line PT67 was obtained from Takara Bio Europe/Clontech. Cells were maintained in a humidified incubator at 37°C in 5% to 8% CO_2 atmosphere in RPMI-1640 or Dulbeccos' Modified Eagle's Media (DMEM; both Invitrogen) containing 10% heat-inactivated FBS (Biochrom) and 100 μg/mL gentamicin (Invitrogen). Cell lines were checked routinely for purity (e.g., EWS-FLI1 translocation product, surface antigen, or HLA-phenotype) and mycoplasma contamination.

RNA interference

For transient RNA interference (RNAi), cells were transfected with siRNAs as described previously (17). siRNA sequences are provided in the Supplementary Information.

Constructs and retroviral gene transfer

For stable silencing of DKK2 expression, oligonucleotides were designed corresponding to the most efficient siRNA used for transient RNAi (see Supplementary Information), and retroviral gene transfer was conducted as described previously (17).

Quantitative RT-PCR

Differential gene expression was analyzed by quantitative RT-PCR (qRT-PCR) using TaqMan Universal PCR Master Mix and fluorescence detection with an AB 7300 Real-Time PCR System (both Applied Biosystems) as described previously (17). A list of the assays used is provided in the Supplementary Information.

Flow cytometry

For DNA content, cells were fixed in ice-cold 70% ethanol at −20°C overnight and stained with propidium iodide (50 mg/mL) plus RNase (5 mg/mL) in PBS. The fluorescence of cells was measured using a FACSCalibur flow cytometer (BD Biosciences) and analyzed using CellQuest software (BD Biosciences).

Proliferation assay

Cell proliferation was measured with an impedance-based instrument system (xCELLigence, Roche/ACEA Biosciences) enabling label-free real time cell analysis. Briefly, 1×10^4 to 3×10^4 cells were seeded into 96-well plates with 200 μL media containing 10% FBS and allowed to grow up to 72 hours. Cellular impedance was measured periodically every 4 hours, and gene knockdown was monitored by qRT-PCR.

Colony-forming assay

Cells were seeded in duplicate into a 35-mm plate at a density of 5×10^3 cells per 1.5-mL methylcellulose-based media (R&D Systems) according to the manufacturer's instructions and cultured for 10 to 14 days at 37°C/5% CO_2 in a humidified atmosphere.

In vitro invasion assay

To study cell invasion, the BioCoat Angiogenesis System: Endothelial Cell invasion was used (BD Biosciences) according to the manufacturer's instructions as described previously (18).

Western blot

Procedures were described previously (17). Following antibodies were used: anti-DKK2 (1:100; PAB3570, Abnova), anti-GAP43 (1:500; ab7462; Abcam), and horseradish peroxidase (HRP)-coupled bovine anti-rabbit IgG (1:500; sc-2370; Santa Cruz Biotechnology). Equal protein loading was controlled with rabbit polyclonal to HPRT antibodies (1:500; sc20975; Santa Cruz Biotechnology).

Differentiation assay

For neuron/astrocyte-like cell differentiation, cells were cultured as already described (17), and the differentiated cells were identified by staining with an antibody directed against GFAP (BD Biosciences) and visualized with a fluorescein isothiocyanate (FITC)-labeled goat anti-mouse F(ab')2 fragment (Jackson ImmunoResearch Laboratories) or with an antibody against the neuronal marker GAP43 (Abcam) using Western blot analysis.

Microarray data

Comparative gene expression analysis was conducted as previously described (17, 18) using human Gene ST arrays (Affymetrix, GSE36100). Gene set enrichment analysis (GSEA) and set-to-set pathway analyses of leading-edge genes were

Published OnlineFirst November 30, 2012; DOI: 10.1158/0008-5472.CAN-12-1492

conducted with the GSEA tool (http://www.broad.mit.edu/gsea) in default parameters (19).

Animal model

Immunodeficient Rag2$^{-/-}\gamma c^{-/-}$ mice on a BALB/c background were obtained from the Central Institute for Experimental Animals (Kawasaki, Japan) and maintained in our animal facility under pathogen-free conditions in accordance with the Institutional Guidelines and approval by local authorities. Immunodeficient NOD/SCID Balb/c mice were purchased by Charles River Laboratories International. Experiments were carried out in 6- to 16-week-old mice.

In vivo experiments

For the analysis of *in vivo* tumor growth and metastatic potential, 1.5×10^6 to 3×10^6 Ewing sarcoma cells and derivates were injected in a volume of 0.2 mL into immunodeficient Rag2$^{-/-}\gamma c^{-/-}$ or NOD/SCID Balb/c mice as described previously (17, 18). To examine bone invasiveness and osteolysis, mice were anesthetized with 500 mg/mL Novaminsulfon (Ratiopharm) and isoflurane (Abbott). A 30-gauge needle was introduced through the proximal tibia plateau, and 2×10^5 Ewing sarcoma cells in a volume of 20 μL were injected into the medullary cavity. In all experiments, tumors and affected tissues were recovered and processed for histologic analyses. Intratibial tumor formation was monitored by X-ray radiography.

Histology

Murine organs were fixed in phosphate-buffered 4% formaldehyde and embedded in paraffin. Three- to 5-μm thick sections were stained with hematoxylin and eosin (H&E). The amount of osteoclasts was detected by tartrate-resistant acid phosphatase (TRAP) staining. All sections were reviewed and interpreted by 2 pathologists (J. Calzada-Wack and I. Esposito).

Statistical analyses

Data are mean ± SEM as indicated. Differences were analyzed by unpaired 2-tailed Student's *t* test as indicated using Excel (Microsoft) or Prism 5 (GraphPad Software); $P < 0.05$ was considered statistically significant (*, $P < 0.05$; **, $P < 0.005$; ***, $P < 0.0005$).

Results

DKK2 is highly overexpressed in Ewing sarcomas

In a previous microarray analysis, we identified *DKK2* as 1 of 37 genes, which were strongly upregulated in Ewing sarcoma compared with normal tissues (Fig. 1A; ref. 8). To analyze specificity of DKK2 expression in Ewing sarcoma, we tested Ewing sarcoma cell lines against a series of different osteosarcoma and neuroblastoma cell lines. qRT-PCR revealed a high expression of DKK2 only in bone-associated tumors such as Ewing sarcoma and osteosarcomas but not in neuroblastomas and other small round blue cell tumors (Fig. 1B and Supplementary Fig. S1).

Although DKK2 seems upregulated in several pediatric bone tumors, we were curious whether DKK2 expression in Ewing sarcoma is dependent on the expression of the oncofusion protein EWS-FLI1. Transient knockdown of EWS-FLI1 by specific siRNA did not significantly affect DKK2 expression in 4 Ewing sarcoma cell lines, indicating DKK2 expression in Ewing sarcoma to be independent of EWS-FLI1 (Fig. 1C). Furthermore, constitutive suppression of DKK2 did not influence EWS-FLI1 mRNA levels (Fig. 1D).

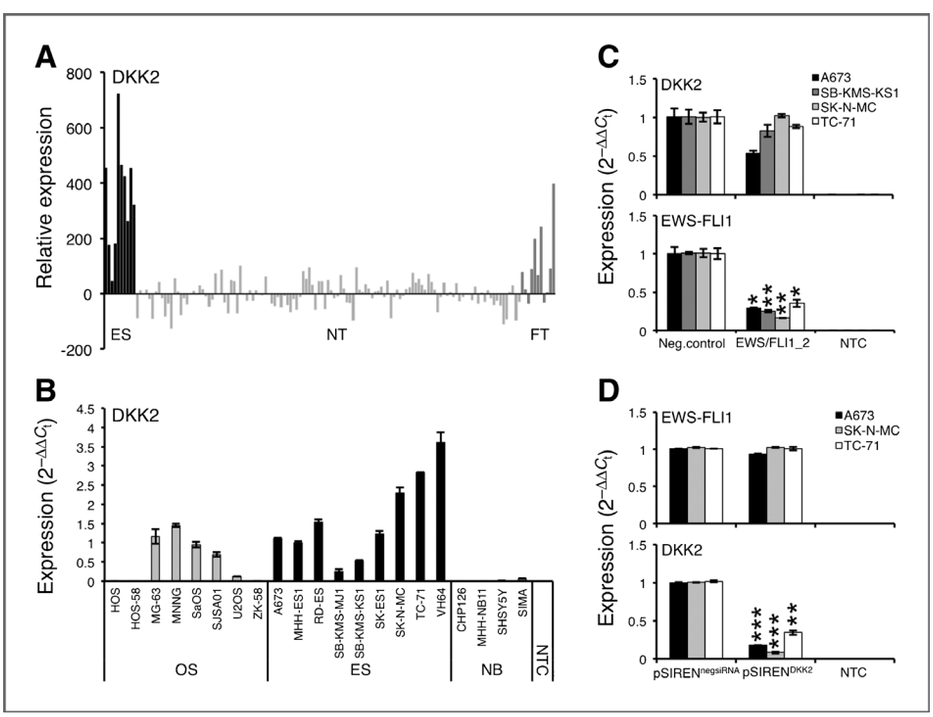

Figure 1. DKK2 is highly overexpressed in Ewing sarcomas. A, expression profile of DKK2 in Ewing sarcoma in comparison to normal tissue (NT) and fetal tissue (FT). Ewing sarcoma and NT samples were analyzed using EOS-Hu01 microarrays (8). B, DKK2 expression in different tumor cell lines analyzed by qRT-PCR. Data are mean ± SEM. C, RNAi of EWS-FLI1 expression (bottom) does not suppress DKK2 RNA expression (top). EWSFLI1_2 represents the specific siRNA (neg. control, nonsilencing siRNA). Results of qRT-PCR 48 hours after transfection are shown. Data are mean ± SEM of 2 independent experiments; *t* test. NTC, nontemplate control. D, analysis of DKK2 and EWS-FLI1 expression after constitutive DKK2 knockdown using qRT-PCR. Data are mean ± SEM of 2 independent experiments; *t* test. NTC, nontemplate control.

Published OnlineFirst November 30, 2012; DOI: 10.1158/0008-5472.CAN-12-1492

DKK2 increases tumor growth and metastasis *in vitro* and *in vivo*

To analyze the impact of DKK2 overexpression on the phenotype of Ewing sarcoma, we transiently and constitutively downregulated DKK2 in 3 different Ewing sarcoma cell lines (Fig. 2A and B). Using an xCELLigence instrument, we first analyzed the effect of DKK2 knockdown on the proliferation of Ewing sarcoma cell lines *in vitro*. Constitutive downregulation of DKK2 revealed a significant inhibition of proliferation in A673 and SK-N-MC cells (Fig. 2C), without significantly affecting cell-cycle progression (Fig. 2D). We next tested anchorage-independent growth of stable DKK2 infectants in methylcellulose. As shown in Fig. 2E, constitutive DKK2 knockdown clearly reduced colony formation in all 3 Ewing sarcoma cell lines in a dose-dependent manner (Fig. 2B).

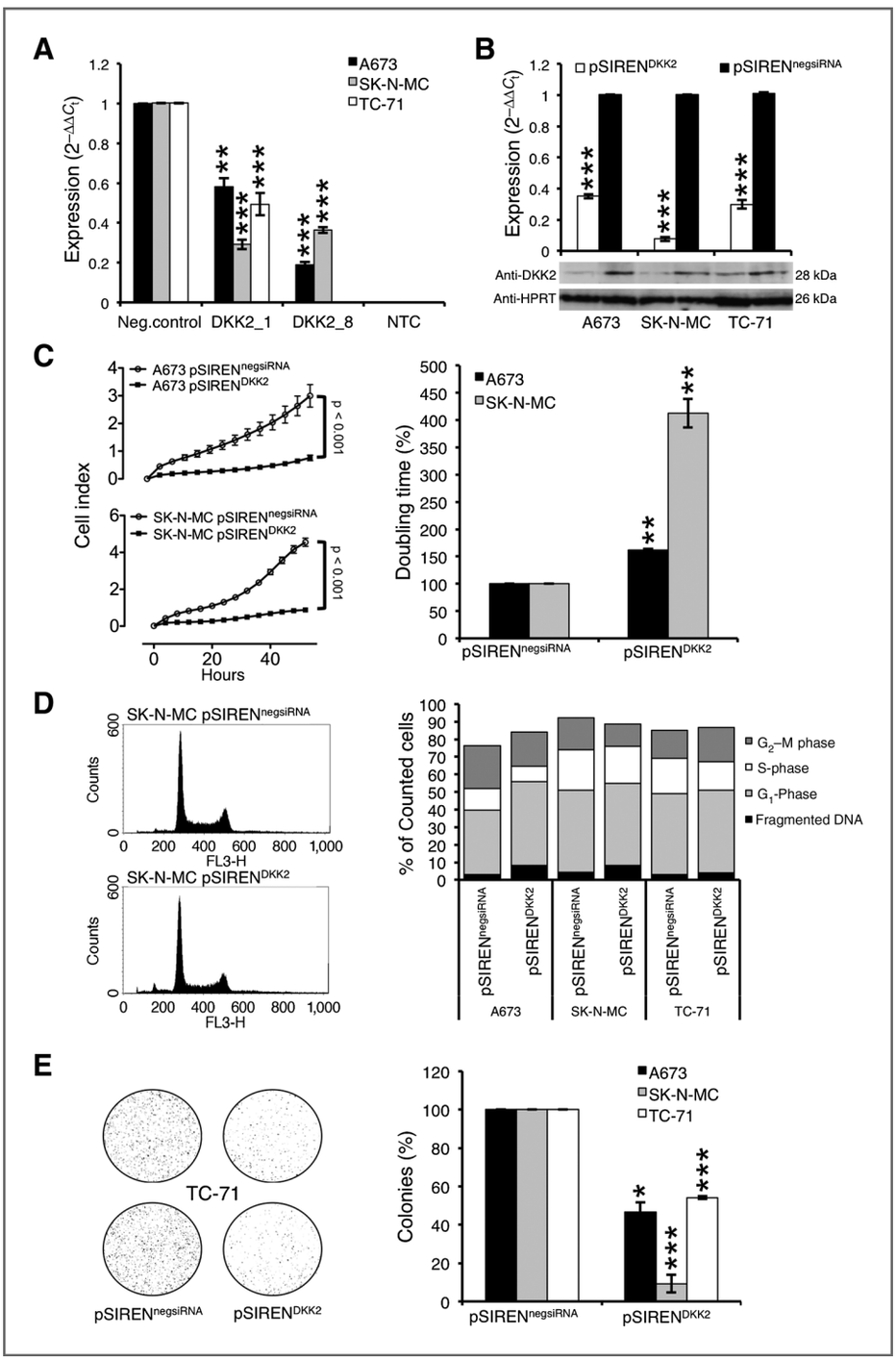

Figure 2. DKK2 knockdown influences *in vitro* growth. A, transient transfection of Ewing sarcoma cell lines with different specific siRNAs. Knockdown efficacy was tested by qRT-PCR 72 hours after transfection. Data are mean ± SEM of 3 independent experiments; *t* test. NTC, nontemplate control. B, constitutive suppression of DKK2 expression after infection of Ewing sarcoma cells with DKK2 specific shRNA constructs as measured by qRT-PCR and Western blot analysis (pSIREN^{DKK2}, control: pSIREN^{negsiRNA}). qRT-PCR data are mean ± SEM of 20 independent experiments; *t* test. NTC, nontemplate control. C, left, analysis of proliferation of constitutively infected Ewing sarcoma cell lines with xCELLigence. Cellular impedance was measured every 4 hours (relative cell index). Data are mean ± SEM (hexaplicates/group); *t* test. Right, doubling time of constitutive A673 and SK-N-MC DKK2 shRNA infectants. Data are mean ± SEM of 2 independent experiments/cell line (hexaplicates/group); *t* test. D, summary of 2 independent cell-cycle distribution analyses of shRNA infectants by propidium iodine staining and flow cytometry. E, analysis of anchorage-independent colony formation in methylcellulose of Ewing sarcoma cell lines with stable DKK2 knockdown (pSIREN^{DKK2}). Left, macrographs show a representative experiment with TC-71. Right, data are mean ± SEM of 3 independent experiments (duplicates/group); *t* test.

Published OnlineFirst November 30, 2012; DOI: 10.1158/0008-5472.CAN-12-1492

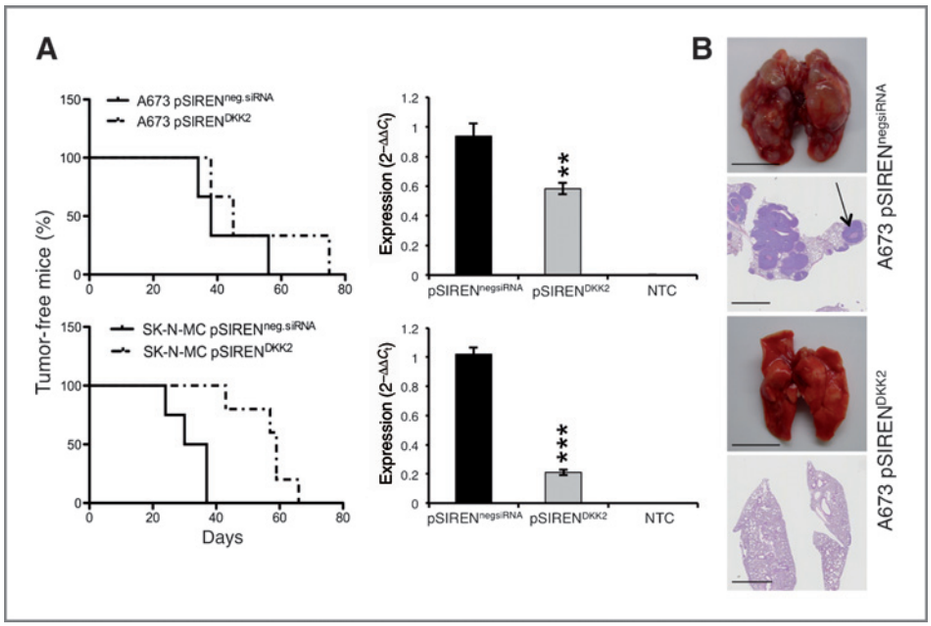

Figure 3. DKK2 increases local tumor growth and metastasis *in vivo*. A, left, evaluation of tumorigenicity of constitutive A673 and SK-N-MC DKK2 shRNA infectants in immunodeficient mice (3–5 mice/group). Right, post *ex vivo* DKK2 expression using qRT-PCR. Data are mean ± SEM, *t* test. B, analysis of metastatic potential of A673 and SK-N-MC with stable DKK2 knockdown and controls (pSIREN^{negsiRNA}; 4 mice/group). The top 2 panels show lung with extensive metastases (arrow) and the bottom 2 panels depict lung without metastases after A673 pSIREN^{DKK2} injection (H&E; scale bar, 5 or 2 mm).

We further examined whether suppression of DKK2 in Ewing sarcoma affects tumorigenicity and metastasis *in vivo*. We injected stable pSIREN^{DKK2}-infected A673 and SK-N-MC cells and respective controls subcutaneously into the inguinal region of immunodeficient mice and analyzed tumor growth. As shown in Fig. 3A, DKK2 knockdown clearly delayed local tumor growth in both Ewing sarcoma cell lines in a dose-dependent manner. Similarly, suppression of DKK2 significantly reduced the number of lung metastases, when cells were injected into the tail veins of Rag2$^{-/-}\gamma c^{-/-}$ mice (Fig. 3B). Furthermore, considering in addition liver and kidney metastases, pSIREN^{DKK2} infectants revealed a strong reduction of overall metastatic potential by up to 95.8% (Table 1), suggesting a critical role of DKK2 in Ewing sarcoma growth and metastasis.

DKK2 knockdown inhibits invasiveness regulated by MMP1 *in vitro*

To identify possible DKK2 downstream targets that are presumably involved in metastasis, we transiently downregulated DKK2 in A673 and SK-N-MC cells (Fig. 2A) and compared their expression pattern with pSIREN^{negsiRNA} cells in a microarray analysis on human Gene ST arrays (Affymetrix, GSE36100). Considering a minimum linear fold change more than ±1.5, we identified 281 differentially regulated genes of which 207 genes were downregulated after DKK2 knockdown (Fig. 4A). Differential expression of 5 of these genes, which all have been reported to be involved in cellular invasiveness and migration, was confirmed by qRT-PCR (Fig. 4B). The only upregulated gene of these 5 genes is the key cell–cell adhesion molecule *E-Cadherin* (*CDH1*), which is a well-established antagonist of invasion and metastasis (20). The 4 downregulated genes are the *integral cell membrane glycoprotein CD44*, which has a postulated role in matrix adhesion and migration (21, 22), the *cellular adhesion molecule 1* (*ICAM1*), which is important for endothelial transmigration into tissues (23), and the matrix metalloproteinases *MMP1* and *MMP7*, both with crucial roles in migration and invasion (24–26). In this context, stably DKK2-silenced Ewing sarcoma cells showed significantly reduced invasiveness when subjected to Matrigel-covered

Table 1. Total number of apparent metastases

	A673		SK-N-MC	
	pSIREN^{negsiRNA}	pSIREN^{DKK2}	pSIREN^{negsiRNA}	pSIREN^{DKK2}
Liver	12	2	135	8
Lung	366	14	0	0
Kidney	2	0	0	0

NOTE: Quantitative evaluation of metastasis: all macroscopically visible metastases in lungs, livers, and kidneys were counted and confirmed by histology after injection with A673 pSIREN^{negsiRNA} and pSIREN^{DKK2} cells.

Published OnlineFirst November 30, 2012; DOI: 10.1158/0008-5472.CAN-12-1492

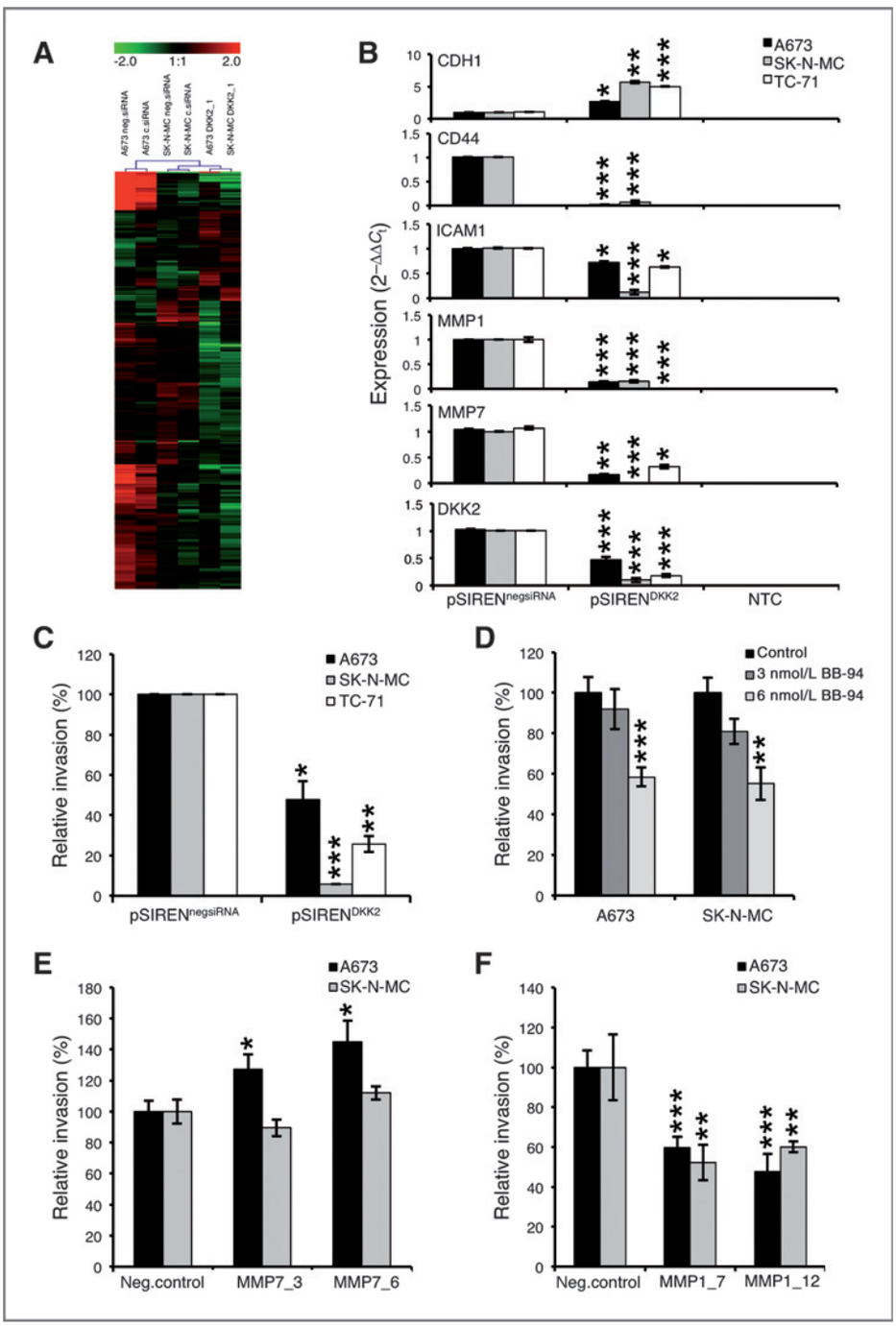

Figure 4. DKK2 knockdown suppresses invasiveness regulated by MMP1. A, microarray data of selected genes after transient DKK2 knockdown (GSE36100). B, confirmation of the array results for selected genes presumably influencing invasiveness with constitutive DKK2 knockdown infectants using qRT-PCR. (*CDH1*, *CD44*, *ICAM1*, *MMP1*, *MMP7*, *DKK2*). Data are mean ± SEM of 3 independent experiments; *t* test. NTC, nontemplate control. C, analysis of invasiveness of Ewing sarcoma cell lines through Matrigel after transfection with specific DKK2 shRNA constructs. Data are mean ± SEM of 2 independent experiments; *t* test. D, analysis of invasiveness of A673 and SK-N-MC treated with 3 or 6 nmol/L of the MMP inhibitor Batimastat (BB-94) or vehicle. Data are mean ± SEM of 2 independent experiments; *t* test. E and F, invasiveness of A673 and SK-N-MC after transfection with 2 specific MMP1 (5F) or MMP7 (5E) siRNAs 48 hours before seeding. Data are mean ± SEM; *t* test.

Transwell assays (BioCoat Angiogenesis System; Fig. 4C). As previously reported, MMPs seems to be important for Ewing sarcoma invasiveness (18). Therefore, we examined the invasiveness of A673 and SK-N-MC cells after treatment with 3 or 6 nmol/L Batimastat (BB-94)—a specific MMP inhibitor. As expected, treatment with BB-94 prominently reduced the amount of cells crossing the Matrigel (Fig. 4D). We next transiently knocked down MMP1 or MMP7, each with 2 different specific siRNAs. As shown in Fig. 4E and F, only knockdown of MMP1, but not of MMP7, reduced invasiveness of Ewing sarcoma cells, suggesting that the reduced invasive potential of DKK2-silenced Ewing sarcoma cells is mediated—at least in part—via MMP1.

DKK2 decreases neuronal differentiation *in vitro*

Subsequent GSEA of our microarray data identified 75 differentially regulated gene sets [normalized enrichment score (NES) < −1.54 or NES > 1.30], that belong to 1 of the

Published OnlineFirst November 30, 2012; DOI: 10.1158/0008-5472.CAN-12-1492

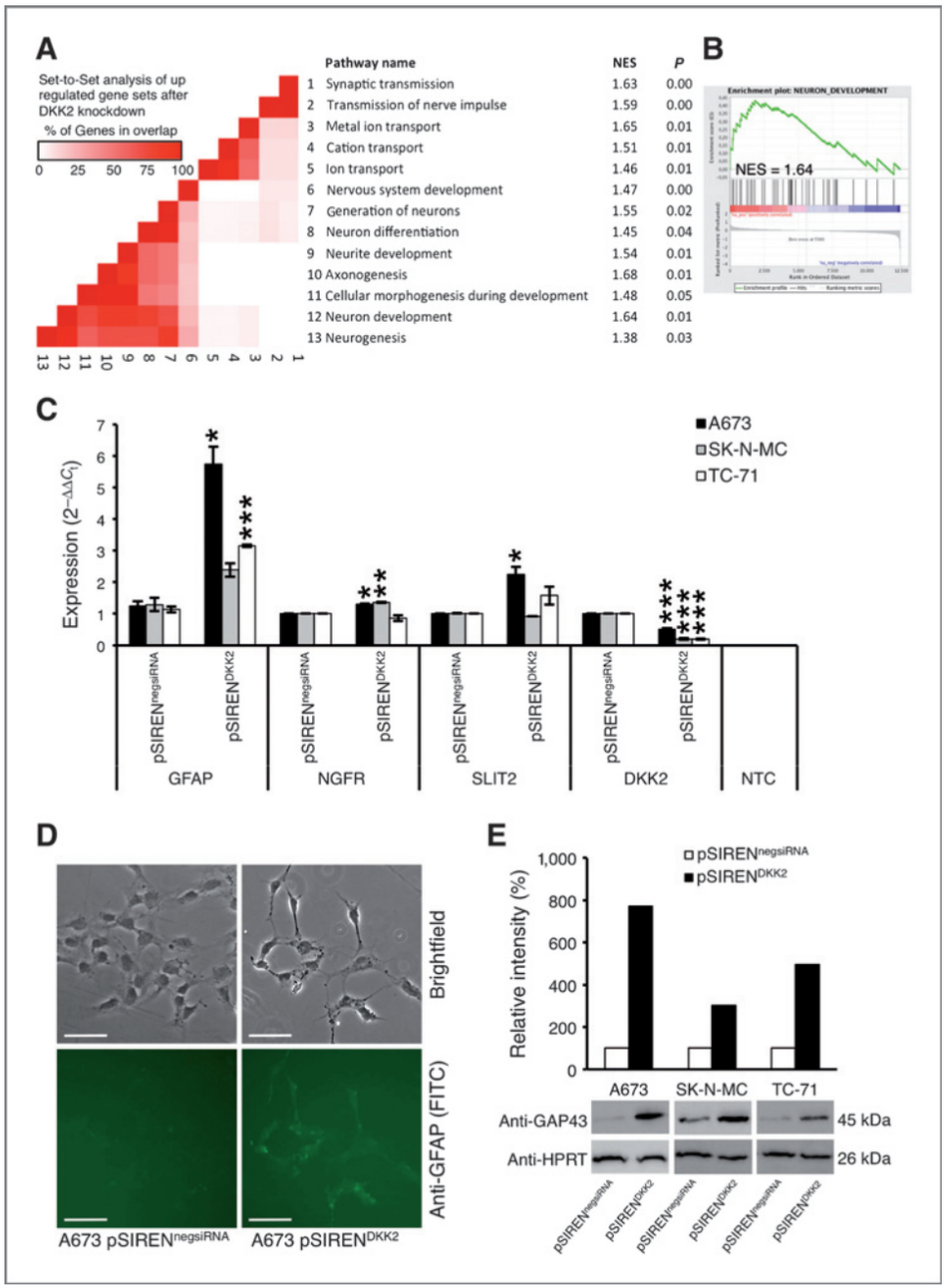

Figure 5. DKK2 knockdown increases neuronal differentiation. A, GSEA leading-edge analysis of identified gene sets upregulated by transient DKK2 knockdown (GSEA; C5_all, GO gene sets). Set-to-set analysis shows a correlation between DKK2 knockdown and upregulation of neuronal differentiation genes. B, GSEA enrichment plot of one representative gene set after constitutive suppression of DKK2. C, qRT-PCR of different neuronal marker genes after stable DKK2 knockdown. (*GFAP*, *NGFR*, *SLIT2*, *DKK2*). Data are mean ± SEM of 2 independent experiments; *t* test. NTC, nontemplate control. D, analysis of neurogenic differentiation of stable A673 infectants pSIREN^{DKK2} and pSIREN^{negsiRNA} treated for 6 days with 0.1 mmol/L BHA. Immunofluorescent staining of GFAP is shown (scale bar, 500 μm). Similar results were obtained with SK-N-MC and TC-71. E, evaluation of the differentiation potential after neurogenic differentiation of Ewing sarcoma cell lines constitutively transfected with DKK2 shRNA treated for 6 days with 0.1 mmol/L BHA shown by Western blot analysis with GAP43 antibody and corresponding densitometry (top). Hypoxanthine guanine phosphoribosyltransferase (HPRT) was used as loading control.

3 ontologies: molecular function, cellular component, or biologic processes (C5: GO gene sets, v3.0; ref. 27). Set-to-set analysis of leading-edge top ranked downregulated gene sets (C5_all, v3.0) revealed a strong overrepresentation of gene sets involved in anti-apoptotic pathways (Supplementary Fig. S2A–S2C) that possibly explains the slightly higher rate of dead cells after DKK2 knockdown *in vitro* and *in vivo* (Fig. 2D, sub-G_1 fraction; data not shown). Consistently, DKK2 knockdown increased the rates of apoptosis as measured by Annexin-V and 7-aminoactinomycin D (7-AAD) staining (Supplementary Fig. S2D). Moreover, the set-to-set analysis of the upregulated gene sets (C5_all, v3.0) revealed a strong overrepresentation of gene sets involved in neuronal differentiation and development (Fig. 5A and B). To verify this prediction, we first examined the overexpression of 3 leading-edge genes, which are all involved in neurogenesis, namely, *glial fibrillary acidic protein* (*GFAP*), *nerve growth factor receptor* (*NGFR*), and *slit, drosophila, homolog of, 2* (*SLIT2*), using qRT-PCR (Fig. 5C). Subsequently, we induced neurogenic differentiation with 0.1 mmol/L BHA in 2% dimethyl sulfoxide (DMSO) in stable A673, SK-N-MC, and TC-71 DKK2 short hairpin RNA (shRNA) infectants. We observed that Ewing sarcoma cell lines were able to fully differentiate and express GFAP, a major intermediate filament protein of mature astrocytes (28), only after DKK2

Published OnlineFirst November 30, 2012; DOI: 10.1158/0008-5472.CAN-12-1492

suppression (Fig. 5D). Similarly growth-associated protein 43 (GAP43), a protein exclusively expressed on the synaptosomal membrane of nerve tissues (29), was significantly higher expressed in Ewing sarcoma cells after DKK2 knockdown, as shown in Fig. 5E, indicating that DKK2 inhibits the neuronal differentiation potential of Ewing sarcoma cells.

DKK2 enhances bone invasion and osteolysis *in vivo*

We next investigated whether DKK2 can influence their differentiation potential toward other tissues or lineages. Min and colleagues already showed that DKK2 promotes angiogenesis (30), therefore, we examined the endothelial differentiation capacity of Ewing sarcoma cells, but we did not detect any differences between cells with/without DKK2 knockdown in tube formation assays (Supplementary Fig. S3A and S3B). Moreover, given that DKK2 is also implicated in terminal osteoblast differentiation (14, 16) and osteoclastogenesis (14, 15), we subsequently analyzed the ability of Ewing sarcoma cells to differentiate along bone lineages. As shown in Supplementary Fig. S4, induction of chondrogenic and osteogenic differentiation with specific growth media was clearly impaired in DKK2 knockdown cells. Furthermore, we examined the differential expression of key players associated with bone colonization in stable DKK2 infectants. We chose *chemokine, CXC motif, receptor 4* (*CXCR4*), *parathyroid hormone-like hormone* (*PTHrP*), *RUNT-related transcription factor 2* (*RUNX2*), and *transforming growth factor beta-1* (*TGFβ1*) for follow-up due to their involvement in preparing the premetastatic niche, homing, and invasion to bone, as well as their role in local and metastatic tumor growth in bones (26). We could show that the expression of these genes was significantly reduced in Ewing sarcoma cells with constitutive DKK2 knockdown compared with controls (Fig. 6A). Interestingly, 3 of the 5 genes are also involved in the osteolytic behavior of tumor cells (26), which seems important as Ewing sarcoma are well-known osteolytic tumors. To verify this observation, we further analyzed the expression of other genes associated with osteolysis, namely *hypoxia-inducible factor 1, alpha subunit* (*HIF1α*), *jagged 1* (*JAG1*), *interleukin 6* (*IL6*), and *vascular endothelial growth factor receptor 1* (*VEGF*; ref. 26). As expected, knockdown of DKK2 significantly reduced the expression of these genes (Fig. 6B)

On the basis of these results, we analyzed whether suppression of DKK2 has a role in the process of bone invasion and osteolysis *in vivo*. We injected constitutively DKK2 silenced A673 cells into the tibiae of immunodeficient Rag2$^{-/-}\gamma c^{-/-}$ mice and analyzed bone infiltration and destruction by X-ray radiography and histology. As shown in Fig. 6C–F, DKK2 knockdown significantly reduced bone infiltration and osteolysis. Only 25% of the mice injected with A673 pSIREN^{DKK2} cells exhibited an infiltration of tumor cells into bone, whereas bone invasion was observed in 87.5% of the respective controls (Fig. 6D). The pSIREN^{DKK2}-mediated lesions were smaller and less destructive than the lesions caused by control cells, as measured by the amount of TRAP-positive osteoclasts in the tumor (Fig. 6E and F). In addition, pilot screening of human Ewing sarcoma samples suggested the level of DKK2 expression to be associated with invasive growth and survival (Supplementary Fig. S5), although a careful retrospective study here is necessary to obtain significant results.

In summary, these data show that DKK2 critically influences the differentiation process of Ewing sarcoma cells along the chondrogenic and osteogenic lineage and is crucial for Ewing sarcoma bone invasion and osteolysis *in vitro* and *in vivo*.

Discussion

Ewing sarcoma are osteolytic bone tumors, characterized by early metastasis into lungs and bones (2). In the present study, we identified DKK2 as a highly overexpressed protein in Ewing sarcoma that seems critically involved in the malignant behavior of this disease, presumably, in part, via the activation of Wnt/β-catenin signaling (Supplementary Fig. S6). Our data support a role of DKK2 overexpression for the maintenance of Ewing sarcoma osteolysis, bone invasiveness, and metastatic spread, associated with a reprograming from neuronal to chondro-osseous differentiation. Furthermore, we showed that DKK2 is also important for anchorage-independent colony formation and proliferation of Ewing sarcoma cells *in vitro* and for tumorigenicity *in vivo*. High expression of DKK2 in Ewing sarcoma raises the question whether DKK2 expression is dependent on the oncogenic fusion protein EWS-FLI1, as reported by Miyagawa and colleagues (31). However, in line with the findings of Navarro and colleagues (32), we found that the expression of DKK2 is mostly independent of EWS-FLI1.

Our functional analyses suggest that in Ewing sarcoma, MMP1 but not MMP7 is responsible for the reduced invasiveness after DKK2 knockdown *in vitro*. MMP1 as well as MMP7 are known to be involved in bone invasion and bone metastasis (24–26), although this finding does not preclude other DKK2 driven factors to be relevant for invasiveness and metastasis. One possible alternative candidate is E-cadherin, a key cell–cell adhesion molecule, which is upregulated after DKK2 knockdown and which has a strong anti-invasive and antimetastatic role in tumor progression (20). In Ewing sarcoma, it mainly seems to suppress anoikis through activation of *ERBB4*; however, this gene is not enhanced after DKK2-mediated CDH1 increase (data not shown; ref. 33). Other genes associated with invasion and metastasis are suppressed after DKK2 knockdown such as *CD44*—an integral cell membrane glycoprotein. As CD44 promotes cell proliferation, invasion, and migration and further inhibits apoptosis, its downregulation after DKK2 knockdown may, in part, explain the increase of cell death observed in our study (21, 22, 34). In addition, invasion in Ewing sarcoma cells may also be promoted by the intercellular adhesion molecule 1 (ICAM1), which is important for the extravasation of circulating tumor cells during metastasis (23). Of note, 4 of our 5 validated DKK2 target genes are associated with bone colonization, bone invasion, and osseous differentiation, which is interesting in the pathophysiologic context of Ewing sarcoma that frequently arise in and metastasize into bones.

In recent years, some genes were identified that enabled bone metastasis of different tumor entities. Among them are *secreted phosphoprotein 1* (*OPN*; ref. 35), a potent ligand of CD44

Published OnlineFirst November 30, 2012; DOI: 10.1158/0008-5472.CAN-12-1492

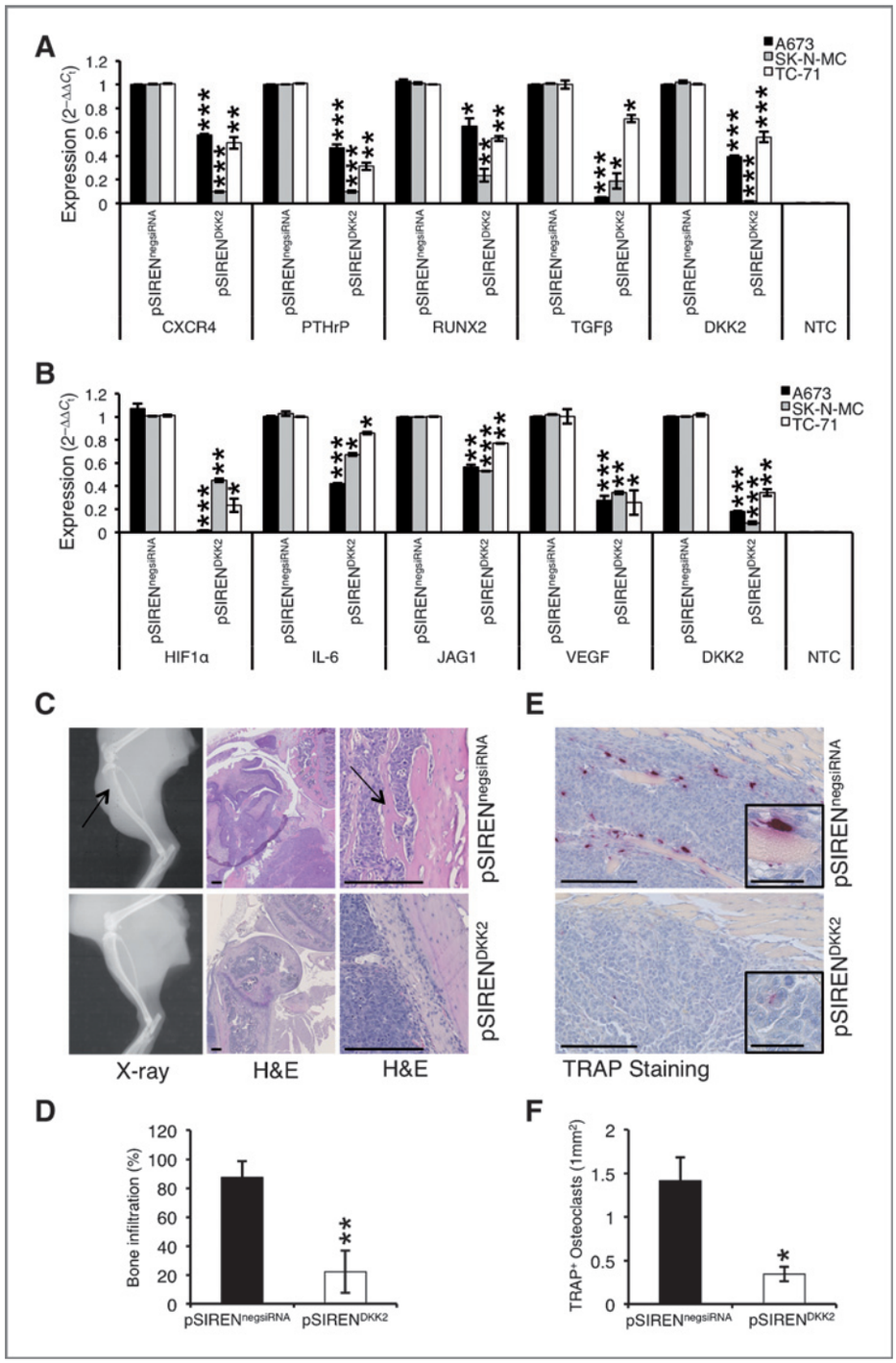

Figure 6. DKK2 enhances bone invasiveness and osteolysis. A, qRT-PCR of Ewing sarcoma cell lines with stable DKK2 knockdown. (*CXCR4*, *PTHrP*, *RUNX2, TGFβ*, *DKK2*). Data are mean ± SEM of 3 independent experiments; *t* test. NTC, nontemplate control. B, mRNA expression analyses of known osteolytic genes after constitutive DKK2 knockdown using qRT-PCR (*HIF1α*, *IL6*, *JAG1*, *VEGF*, *DKK2*). Data are mean ± SEM of 2 independent experiments; *t* test. NTC, nontemplate control. C–F, analysis of bone invasiveness and osteolysis of constitutive A673 DKK2 shRNA infectants and negative controls in an orthotopic bone xenotransplantation model (9 mice/group). Affected bones were assessed by X-ray radiography and histology. C, A673 pSIREN^{DKK2} cells caused significantly less tumor infiltration into bone when compared with A673 pSIREN^{negsiRNA}, where tumor cells destroyed the cortical bone (arrows) and generated extra tumor mass outside the bone (X-ray, H&E; scale bar, 0.25 mm). D, percentage of mice exhibiting bone infiltration after intratibial injection. Data are mean ± SEM; *t* test (**, $P < 0.003$). E, TRAP staining of osteoclasts to quantify osteolysis. Scale bar, 0.25 and 0.05 mm (insets). F, average number of TRAP$^+$ osteoclasts (1 mm^2; 3 tumor samples/group; *t* test).

(22), *cbp/p300-interacting transactivator, with glu/asp-rich c-terminal domain, 2* (*CITED2*; ref. 36), *cAMP response element-binding protein 1* (*CREB1*; ref. 37), and *secreted protein, acidic, cysteine-rich* (*SPARC*; ref. 38). Interestingly, CD44 and OPN as well as the target genes of CITED2 (*MMPs*, *TGFβ1*, *PTHrP*), CREB1 (*MMPs*, *PTHrP*), and SPARC (*VEGF*) are also regulated by DKK2, as shown in this study. Moreover, we showed that DKK2 modulates the expression of additional genes important for osteolysis (*CXCR4*, *HIF1α*, *JAG1*, *IL6*, *PTHrP*, and *VEGF*). Furthermore, high CXCR4 expression seems associated with poor prognosis in patients with Ewing sarcoma (39). The transcription factor RUNX2 affects cancer cell invasion and osteolysis (26) and can bind to the oncogenic fusion protein EWS-FLI1 (40). This interaction is potentially fostered by a

Published OnlineFirst November 30, 2012; DOI: 10.1158/0008-5472.CAN-12-1492

DKK2-dependent RUNX2 induction and thus promotes the differentiation of Ewing sarcoma cells (40). This could explain the increased neuronal differentiation of Ewing sarcoma cells after DKK2 knockdown showing that not only EWS-FLI1–driven histone methyltransferase EZH2 influences the differentiation potential in Ewing sarcoma (17). However, their chondrogenic and osteogenic differentiation capacity is reduced after DKK2 knockdown, which may be again mediated, at least in part, by RUNX2, as this protein promotes osteogenic and chondrogenic differentiation (26, 40, 41). Furthermore, we could show for the first time that reduced osteolysis after DKK2 knockdown *in vivo* is probably mediated by decreased expression of osteolytic genes, which function either directly via the stimulation of osteoclastic bone resorption (PTHrP, IL6, VEGF) or indirectly (HIF1α, JAG1) by increasing the ratio of receptor activator of NF-κB ligand (RANKL) to osteoprotegerin (OPG) to activate the maturation of osteoclast precursors (26, 42). These data in addition might be of clinical relevance as pilot data obtained from human Ewing sarcoma immunohistology indicate the level of DKK2 expression to be associated with tumor invasiveness and survival.

In synopsis, the current study provides evidence that DKK2 is critically involved in Ewing sarcoma pathology, especially in bone-associated tumor growth and metastasis. With DKK2, we could identify a first element for the mechanisms of bone invasiveness and osteolysis in Ewing sarcoma. DKK family members seem likely to be involved in other bone-infiltrating tumors including osteosarcoma as well as breast or prostate cancer (43–45), supporting a critical role of Wnt/β-catenin signaling for bone metastasis. Hence, DKK2 may constitute a promising new drug target in different bone cancers and bone metastasis that can possibly be used to prevent or at least to delay metastasis.

Disclosure of Potential Conflicts of Interest

No potential conflicts of interest were disclosed.

Authors' Contributions

Conception and design: S. Burdach, G.H.S. Richter
Development of methodology: K. Hauer, I. Esposito
Acquisition of data (provided animals, acquired and managed patients, provided facilities, etc.): K. Hauer, J. Calzada-Wack, T.G.P. Grunewald, D. Baumhoer, S. Plehm
Analysis and interpretation of data (e.g., statistical analysis, biostatistics, computational analysis): K. Hauer, J. Calzada-Wack, K. Steiger, T.G.P. Grunewald, D. Baumhoer, S. Plehm, T. Buch, O.P. da Costa, I. Esposito, S. Burdach, G.H.S. Richter
Writing, review, and/or revision of the manuscript: K. Hauer, J. Calzada-Wack, T.G.P. Grunewald, D. Baumhoer, O.P. da Costa, I. Esposito, S. Burdach, G.H.S. Richter
Administrative, technical, or material support (i.e., reporting or organizing data, constructing databases): T. Buch, O.P. da Costa
Study supervision: T. Buch, S. Burdach, G.H.S. Richter

Acknowledgments

The authors thank Colette Berns for expert technical assistance and Uwe Thiel for support and critically reading of the manuscript. Immunodeficient Rag2$^{-/-}\gamma c^{-/-}$ mice were kindly provided by Mamoru Ito (Central Institute for Experimental Animals).

Grant Support

This work was supported by grants from Technische Universität München (KKF_B08–05 to T.G.P. Grunewald and A09–02 to G.H.S. Richter); the Wilhelm-Sander-Stiftung (2009.901.1 to G.H.S. Richter and S. Burdach); is part of the Translational Sarcoma Research Network supported by the BMBF (FK 01GM0870 and 01GM1104B to G.H.S. Richter and S. Burdach); and Deutsche Forschungsgemeinschaft (DFG_GR3728/1–1 to T.G.P. Grunewald, G.H.S. Richter, and S. Burdach; DFG_GR3728/2–1 to T.G.P. Grunewald). Work in I. Esposito laboratory is supported by the National Genome Research Network (NGFNplus, 01GS0850) and in the laboratory of T. Buch by the Deutsche Forschungsgemeinschaft (SFB-TR22).

The costs of publication of this article were defrayed in part by the payment of page charges. This article must therefore be hereby marked *advertisement* in accordance with 18 U.S.C. Section 1734 solely to indicate this fact.

Received April 23, 2012; revised October 16, 2012; accepted October 30, 2012; published OnlineFirst November 30, 2012.

References

1. Lessnick SL, Ladanyi M. Molecular pathogenesis of Ewing sarcoma: new therapeutic and transcriptional targets. Annu Rev Pathol 2012; 7:145–59.
2. Mackintosh C, Madoz-Gúrpide J, Ordóñez JL, Osuna D, Herrero-Martín D. The molecular pathogenesis of Ewing's sarcoma. Cancer Biol Ther 2010;9:655–67.
3. Ewing J. Classics in oncology. Diffuse endothelioma of bone. James Ewing. Proceedings of the New York Pathological Society, 1921. CA Cancer J Clin 1972;22:95–8.
4. Schmidt D, Harms D, Burdach S. Malignant peripheral neuroectodermal tumours of childhood and adolescence. Virchows Arch A Pathol Anat Histopathol 1985;406:351–65.
5. Burdach S, Jürgens H. High-dose chemoradiotherapy (HDC) in the Ewing family of tumors (EFT). Crit Rev Oncol Hematol 2002;41: 169–89.
6. Burdach S, Thiel U, Schöniger M, Haase R, Wawer A, Nathrath M, et al. Total body MRI-governed involved compartment irradiation combined with high-dose chemotherapy and stem cell rescue improves long-term survival in Ewing tumor patients with multiple primary bone metastases. Bone Marrow Transplant 2010;45:483–9.
7. Coleman RE. Clinical features of metastatic bone disease and risk of skeletal morbidity. Clin Cancer Res 2006;12:6243s–9s.
8. Staege MS, Hutter C, Neumann I, Foja S, Hattenhorst UE, Hansen G, et al. DNA microarrays reveal relationship of Ewing family tumors to both endothelial and fetal neural crest-derived cells and define novel targets. Cancer Res 2004;64:8213–21.
9. Katoh M, Katoh M. WNT antagonist, DKK2, is a Notch signaling target in intestinal stem cells: augmentation of a negative regulation system for canonical WNT signaling pathway by the Notch-DKK2 signaling loop in primates. Int J Mol Med 2007;19:197–201.
10. Brott BK, Sokol SY. Regulation of Wnt/LRP signaling by distinct domains of Dickkopf proteins. Mol Cell Biol 2002;22:6100–10.
11. Mao B, Niehrs C. Kremen2 modulates Dickkopf2 activity during Wnt/LRP6 signaling. Gene 2003;302:179–83.
12. Li L, Mao J, Sun L, Liu W, Wu D. Second cysteine-rich domain of Dickkopf-2 activates canonical Wnt signaling pathway via LRP-6 independently of dishevelled. J Biol Chem 2002;277:5977–81.
13. Uren A, Wolf V, Sun Y-F, Azari A, Rubin JS, Toretsky JA. Wnt/Frizzled signaling in Ewing sarcoma. Pediatr Blood Cancer 2004;43:243–9.
14. Fujita K, Janz S. Attenuation of WNT signaling by DKK-1 and -2 regulates BMP2-induced osteoblast differentiation and expression of OPG, RANKL and M-CSF. Mol Cancer 2007;6:71.
15. Tian E, Zhan F, Walker R, Rasmussen E, Ma Y, Barlogie B, et al. The role of the Wnt-signaling antagonist DKK1 in the development of osteolytic lesions in multiple myeloma. N Engl J Med 2003;349:2483–94.
16. Li X, Liu P, Liu W, Maye P, Zhang J, Zhang Y, et al. Dkk2 has a role in terminal osteoblast differentiation and mineralized matrix formation. Nat Genet 2005;37:945–52.
17. Richter GHS, Plehm S, Fasan A, Rössler S, Unland R, Bennani-Baiti IM, et al. EZH2 is a mediator of EWS/FLI1 driven tumor growth and metastasis blocking endothelial and neuro-ectodermal differentiation. Proc Natl Acad Sci U S A 2009;106:5324–9.

Published OnlineFirst November 30, 2012; DOI: 10.1158/0008-5472.CAN-12-1492

18. Grunewald TGP, Diebold I, Esposito I, Plehm S, Hauer K, Thiel U, et al. STEAP1 is associated with the invasive and oxidative stress phenotype of Ewing tumors. Mol Cancer Res 2012;10:52–65.
19. Subramanian A, Tamayo P, Mootha VK, Mukherjee S, Ebert BL, Gillette MA, et al. Gene set enrichment analysis: a knowledge-based approach for interpreting genome-wide expression profiles. Proc Natl Acad Sci U S A 2005;102:15545–50.
20. Hanahan D, Weinberg RA. Hallmarks of cancer: the next generation. Cell 2011;144:646–74.
21. Aruffo A, Stamenkovic I, Melnick M, Underhill CB, Seed B. CD44 is the principal cell surface receptor for hyaluronate. Cell 1990;61:1303–13.
22. Weber GF, Ashkar S, Glimcher MJ, Cantor H. Receptor-ligand interaction between CD44 and osteopontin (Eta-1). Science 1996;271: 509–12.
23. Roland CL, Harken AH, Sarr MG, Barnett CC Jr. ICAM-1 expression determines malignant potential of cancer. Surgery 2007;141:705–7.
24. Lynch CC, Hikosaka A, Acuff HB, Martin MD, Kawai N, Singh RK, et al. MMP-7 promotes prostate cancer-induced osteolysis via the solubilization of RANKL. Cancer Cell 2005;7:485–96.
25. Lu X, Wang Q, Hu G, Van Poznak C, Fleisher M, Reiss M, et al. ADAMTS1 and MMP1 proteolytically engage EGF-like ligands in an osteolytic signaling cascade for bone metastasis. Genes Dev 2009; 23:1882–94.
26. Weilbaecher KN, Guise TA, McCauley LK. Cancer to bone: a fatal attraction. Nat Rev Cancer 2011;11:411–25.
27. Ashburner M, Ball CA, Blake JA, Botstein D, Butler H, Cherry JM, et al. Gene ontology: tool for the unification of biology. The Gene Ontology Consortium. Nat Genet 2000;25:25–9.
28. Reeves SA, Helman LJ, Allison A, Israel MA. Molecular cloning and primary structure of human glial fibrillary acidic protein. Proc Natl Acad Sci U S A 1989;86:5178–82.
29. Benowitz LI, Routtenberg A. GAP-43: an intrinsic determinant of neuronal development and plasticity. Trends Neurosci 1997;20:84–91.
30. Min J-K, Park H, Choi H-J, Kim Y, Pyun B-J, Agrawal V, et al. The WNT antagonist Dickkopf2 promotes angiogenesis in rodent and human endothelial cells. J Clin Invest 2011;121:1882–93.
31. Miyagawa Y, Okita H, Itagaki M, Toyoda M, Katagiri YU, Fujimoto J, et al. EWS/ETS regulates the expression of the Dickkopf family in Ewing family tumor cells. PLoS One 2009;4:e4634.
32. Navarro D, Agra N, Pestaña A, Alonso J, González-Sancho JM. The EWS/FLI1 oncogenic protein inhibits expression of the Wnt inhibitor DICKKOPF-1 gene and antagonizes beta-catenin/TCF-mediated transcription. Carcinogenesis 2010;31:394–401.
33. Kang H-G, Jenabi JM, Zhang J, Keshelava N, Shimada H, May WA, et al. E-cadherin cell-cell adhesion in Ewing tumor cells mediates suppression of anoikis through activation of the ErbB4 tyrosine kinase. Cancer Res 2007;67:3094–105.
34. Park YS, Huh JW, Lee JH, Kim HR. shRNA against CD44 inhibits cell proliferation, invasion and migration, and promotes apoptosis of colon carcinoma cells. Oncol Rep 2012;27:339–46.
35. Bäuerle T, Adwan H, Kiessling F, Hilbig H, Armbruster FP, Berger MR. Characterization of a rat model with site-specific bone metastasis induced by MDA-MB-231 breast cancer cells and its application to the effects of an antibody against bone sialoprotein. Int J Cancer 2005;115:177–86.
36. Lau WM, Weber KL, Doucet M, Chou Y-T, Brady K, Kowalski J, et al. Identification of prospective factors promoting osteotropism in breast cancer: a potential role for CITED2. Int J Cancer 2010; 126:876–84.
37. Son J, Lee J-H, Kim H-N, Ha H, Lee ZH. cAMP-response-element-binding protein positively regulates breast cancer metastasis and subsequent bone destruction. Biochem Biophys Res Commun 2010; 398:309–14.
38. De S, Chen J, Narizhneva NV, Heston W, Brainard J, Sage EH, et al. Molecular pathway for cancer metastasis to bone. J Biol Chem 2003;278:39044–50.
39. Bennani-Baiti IM, Cooper A, Lawlor ER, Kauer M, Ban J, Aryee DNT, et al. Intercohort gene expression co-analysis reveals chemokine receptors as prognostic indicators in Ewing's sarcoma. Clin Cancer Res 2010;16:3769–78.
40. Li X, McGee-Lawrence ME, Decker M, Westendorf JJ. The Ewing's sarcoma fusion protein, EWS-FLI, binds Runx2 and blocks osteoblast differentiation. J Cell Biochem 2010;111:933–43.
41. Sugawara M, Kato N, Tsuchiya T, Motoyama T. RUNX2 expression in developing human bones and various bone tumors. Pathol Int 2011; 61:565–71.
42. Sethi N, Dai X, Winter CG, Kang Y. Tumor-derived JAGGED1 promotes osteolytic bone metastasis of breast cancer by engaging notch signaling in bone cells. Cancer Cell 2011;19:192–205.
43. Hoang BH, Kubo T, Healey JH, Yang R, Nathan SS, Kolb EA, et al. Dickkopf 3 inhibits invasion and motility of Saos-2 osteosarcoma cells by modulating the Wnt-beta-catenin pathway. Cancer Res 2004;64: 2734–9.
44. Bu G, Lu W, Liu C-C, Selander K, Yoneda T, Hall C, et al. Breast cancer-derived Dickkopf1 inhibits osteoblast differentiation and osteoprotegerin expression: implication for breast cancer osteolytic bone metastases. Int J Cancer 2008;123:1034–42.
45. Hall CL, Bafico A, Dai J, Aaronson SA, Keller ET. Prostate cancer cells promote osteoblastic bone metastases through Wnts. Cancer Res 2005;65:7554–60.

Cancer Research
The Journal of Cancer Research (1916–1930) | The American Journal of Cancer (1931–1940)

AACR American Association for Cancer Research

DKK2 Mediates Osteolysis, Invasiveness, and Metastatic Spread in Ewing Sarcoma

Kristina Hauer, Julia Calzada-Wack, Katja Steiger, et al.

Cancer Res 2013;73:967-977. Published OnlineFirst November 30, 2012.